Angewandte Chemie International Edition

DOI: 10.1002/anie.201102146

High-Spin Non-Heme Iron Complex

C–H Bond Activation of Methanol and Ethanol by a High-Spin $Fe^{IV}O$ Biomimetic Complex**

*William A. Donald, Christine J. McKenzie, and Richard A. J. O'Hair**

The selective and efficient activation of strong organic bonds is one of the major goals in chemistry[1] due to the intense interest in developing more cost-effective and environmentally sustainable routes for the industrial production of chemicals.[2] Many biological enzymes containing metal–oxo active site intermediates,[2b,3] including those that contain a non-heme high-spin ($S=2$) $Fe^{IV}{=}O$ active-site intermediate,[4] can mediate reactions of relevance to organic synthesis (e.g., C–H bond hydroxylation, alcohol oxidation, olefin epoxidation, etc.). As a result, there has been considerable interest in preparing and studying novel $Fe^{IV}{=}O$ complexes that can "mimic" these beneficial properties and provide insights into the chemistry of Fe–oxo enzyme active sites.[2b,5] A key challenge is that high-valent Fe^{IV}–oxo complexes in high-spin states[6] are highly reactive. For example, out of a wide range of synthetic $Fe^{IV}{=}O$ complexes that have been reported,[7] only three are high-spin ($S=2$) non-heme $Fe^{IV}{=}O$ complexes,[8] and these have lifetimes that range from 7 s to 2.2 h at 25 °C.[8]

Another approach for studying highly reactive complexes is to generate and investigate such species in the gas phase, where effects of solvent, counterions, and aggregation, which can all lead to degradation of reactive complexes, can either be eliminated, or carefully controlled. Such studies can potentially reveal new types of transition metal mediated reactions, which may uncover important details of reaction mechanisms and direct the development of future condensed-phase catalysts. Although there have been numerous gas-phase studies of Fe–oxo based ions,[9] and $Fe^{III}O^+$ in particular,[9a,b] the chemistry of high-spin non-heme $Fe^{IV}{=}O$ complexes, of the types that have only recently been synthesized in the condensed phase,[8b,c] have not been explored in vacuo leaving a considerable gap[9c,d] between the fundamental gas-phase Fe–oxo studies and the recent advances in condensed-phase high-valent non-heme Fe–oxo coordination chemistry. Herein we report the gas-phase synthesis of the high-spin complex $[(bpg)Fe^{IV}{=}O]^+$ (where bpg^- is *N*,*N*-bis(2-pyridinylmethyl)glycinato$^-$) and its reactions with methanol and ethanol.[10]

Electrospray ionization (ESI) of 100 μM solutions of $[(bpg)Fe(H_2O)OFe(H_2O)(bpg)](ClO_4)_2$[11] dissolved in a 10:90 acetonitrile:CH_2Cl_2 mixture resulted in the formation of a dominant ion at *m*/*z* 320, corresponding to $[(bpg)FeOFe(bpg)]^{2+}$. Collision-induced dissociation (CID) of isolated $[(bpg)FeOFe(bpg)]^{2+}$ (*m*/*z* 320) leads to the formation of a population of ions at *m*/*z* 328 with a stoichiometry that corresponds to that of $[(bpg)Fe^{IV}O]^+$, in addition to an ion at *m*/*z* 312 corresponding to $[(bpg)Fe^{II}]^+$ (Figure 1 a), which is formed through charge separation of the precursor ion [Eq. (1)] in a redox disproportionation reaction.[12]

$$[(bpg)FeOFe(bpg)]^{2+} \xrightarrow{CID} [(bpg)Fe^{IV}O]^{+} + [(bpg)Fe^{II}]^{+} \qquad (1)$$

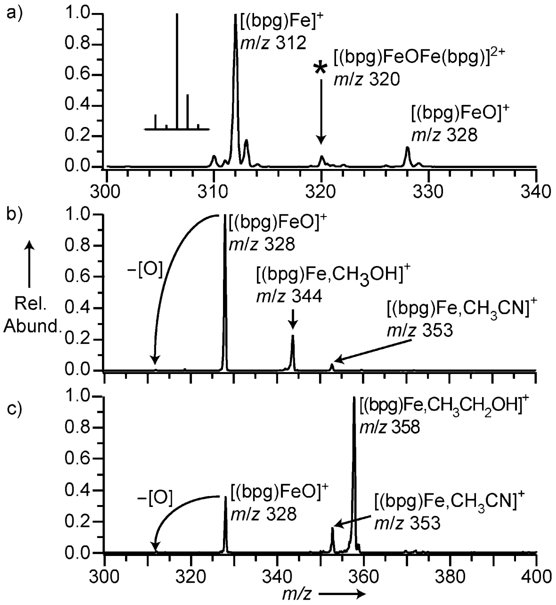

Figure 1. Mass spectra obtained upon a) CID of isolated $[(bpg)FeOFe(bpg)]^{2+}$ (30 ms activation time; 7 *m*/*z* isolation window; theoretical isotope distribution for $[(bpg)Fe]^+$ is given in the inset), b) a 4 s reaction time between isolated $[(bpg)FeO]^+$ (*m*/*z* 328) and methanol (1.2×10^{-6} Torr), and c) a 4 s reaction time between isolated $[(bpg)FeO]^+$ and ethanol (1.0×10^{-6} Torr). Data obtained on linear trap (a) and quadrupole ion trap (b and c; 1.1 *m*/*z* isolation window) mass spectrometers.

---

[*] Dr. W. A. Donald, Prof. R. A. J. O'Hair
School of Chemistry, Bio21 Institute of Molecular Science and Biotechnology, and ARC Centre of Excellence for Free Radical Chemistry and Biotechnology, University of Melbourne
Melbourne, Victoria 3010 (Australia)
E-mail: rohair@unimelb.edu.au
Prof. C. J. McKenzie
Department of Physics and Chemistry
University of Southern Denmark (Denmark)

[**] We thank the Australian Research Council (ARC) for financial support, the Victorian Partnership for Advanced Computing for the allocation of computing resources, and the Danish Council for Independent Research | Natural Sciences. We also thank Dr. G. N. Khairallah for help with modifying the LTQ-FT-ICR mass spectrometer, and Prof. H. Schwarz for providing a preprint of Ref. [10a].

Supporting information for this article is available on the WWW under http://dx.doi.org/10.1002/anie.201102146.

The focus of this work is on the structure and reactivity of the ion of stoichiometry $[Fe,C_{14},H_{14},N_3,O_3]^+$ at m/z 328, which may contain an intact $Fe^{IV}O$ group, or which may have isomerized during the CID process.[13] DFT methods were used to optimize molecular geometries and calculate 0 K energies for several isomers in different electronic spin states. Figure 2 shows the three lowest-energy structures of seven isomers considered: $[(bpg)Fe^{IV}O]^+$ and two $[(bpg\text{-}H)FeOH]^{+\bullet}$ isomers in which a H atom has migrated from the ligand onto the oxygen of the Fe–O group. **2** and **3**, which contain a $Fe^{III}OH$ unit, are substantially lower in energy than the $Fe^{IV}O$ isomer, **1** (by 58 and 25 kJ mol^{-1} for **2** and **3**, respectively). The other four isomers resulting from H-atom abstraction from the pyridine ring of the bpg^- ligand by the $Fe^{IV}O$ unit are all over 50 kJ mol^{-1} higher in energy than the $Fe^{IV}O$ isomer (Supporting Information, Figure S1). All isomers have a central Fe that is ligated through three N atoms and two O atoms in a trigonal bipyrimidal arrangement. The Fe–O bond lengths for the $Fe^{III}OH$ bond for isomers **2** and **3** are 1.8 Å, whereas the $Fe^{IV}{=}O$ bond is calculated to be 1.6 Å, consistent with this bond having more double-bond character than that of the Fe–hydroxide isomers. The calculated $Fe^{IV}{=}O$ bond length for the optimized structure of **1** is essentially the same as that which have been reported for the crystal structures of other non-heme iron(IV)–oxo complexes.[7b,8c,14] The calculated ground state of **1** is the $S=2$ electronic state, which is over 40 and 80 kJ mol^{-1} more stable than the $S=1$ and $S=0$ states, respectively, indicating that **1** has a high-spin ground state.

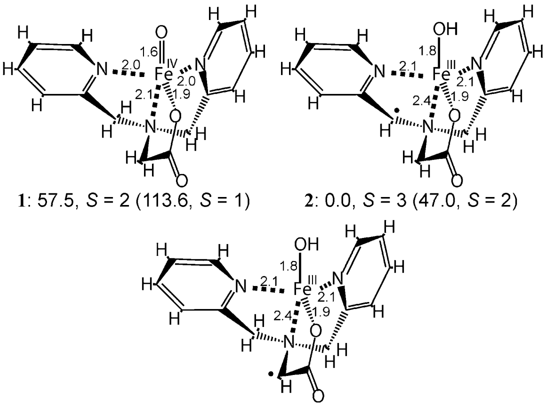

1: 57.5, $S=2$ (113.6, $S=1$) **2**: 0.0, $S=3$ (47.0, $S=2$)

3: 32.5, $S=3$ (81.2, $S=2$)

Figure 2. BP86-optimized structures of possible isomers **1**–**3** ($S=2$ for **1** and $S=3$ for **2** and **3**) for $[Fe,C_{14},H_{14},N_3,O_3]^+$ (m/z 328). B3LYP (0 K) single-point energies are in kJ mol^{-1}, and bond lengths are in Å. Energies for the next-lowest electronic states are given in parentheses. See Supporting Information for details of higher-energy conformers.

To investigate the structure and reactivity of the ion at m/z 328 formed by CID of $[(bpg)FeOFe(bpg)]^{2+}$ [Figure 1a, Eq. (1)], ion–molecule reactions were carried out. This ion reacts with methanol (1.2×10^{-6} Torr) to form product ions with m/z values of 344 and 353 (Figure 1b; 4 s reaction time, precursor depleted by 20%).[15] When ethanol is used under similar conditions, ions with m/z values of 353 and 358 are formed, and the precursor is depleted by approximately 70% (Figure 1c). These data are consistent with the presence of isomer **1** in the m/z 328 ion population, that transfers an O atom to the alcohol to form the coordinatively unsaturated product ion $[(bpg)Fe^{II}]^+$ [Eq. (2)], which subsequently undergoes rapid association reactions with a second alcohol molecule or with acetonitrile from the ESI source [Eq. (3)] (where M = CH_3OH, CH_3CH_2OH, or CH_3CN; and R = H or CH_3).

$$[(bpg)Fe^{IV}O]^+\ (m/z\ 328) + RCH_2OH \rightarrow [(bpg)Fe^{II}]^+\ (m/z\ 312) + H_2O + RCHO \tag{2}$$

$$[(bpg)Fe^{II}]^+\ (m/z\ 312) + M \rightarrow [(bpg)Fe^{II}\ M]^+ \tag{3}$$

The most likely and thermodynamically favored neutral products for the O-atom transfer reaction [Eq. (2)] are a water molecule and the corresponding aldehyde molecule.

Storage of the ion at m/z 328 in the presence of $CH_3{}^{18}OH$ for 4 s results in the formation of ions at m/z 346 and m/z 353 (Figure S2a), which correspond to the formation of $[(bpg)Fe^{II},CH_3{}^{18}OH]^+$ and $[(bpg)Fe^{II},CH_3CN]^+$, respectively. Furthermore, storage of independently generated $[(bpg)Fe]^+$ (from CID of $[(bpg)FeOFe(bpg)]^{2+}$) for 4 s, instead of $[(bpg)FeO]^+$, results in the rapid depletion of $[(bpg)Fe]^+$ and the formation of $[(bpg)Fe,CH_3{}^{18}OH]^+$ and $[(bpg)Fe,CH_3CN]^+$ in nearly the same relative abundance as through the O-atom transfer reaction (Figure S2a vs. S2b). These data suggest that an oxygen atom from $[(bpg)FeO]^+$ is transferred to the alcohol [Eq. (2)], and the resulting product ion $[(bpg)Fe]^+$ can readily form ion–molecule association complexes ($[(bpg)Fe,CH_3{}^{18}OH]^+$ and $[(bpg)Fe,CH_3CN]^+$) [Eq. (3)]. CID of the ion–molecule complexes results in the sole evaporation of the neutral ligand over a wide range of CID conditions.

Under certain conditions, the ion population at m/z 328 can react through another pathway. For example, storage of isolated "$[Fe(bpg)O]^+$" (m/z 328; formed through CID of $[(bpg)FeOFe(bpg)]^{2+}$ for 30 ms) for 2 s in the presence of methanol at a pressure of 0.6×10^{-6} Torr results in the formation of the peaks at m/z values of 312, 342 and 344 (Figure 3a). Isolation and storage of the m/z 342 ion after the 2 s ion–molecule reaction, for 10 ms to 10 s, does not result in the formation of an ion at m/z 312 or m/z 344. The ions at m/z 312 and 344 correspond to the O-atom transfer product ions, $[(bpg)Fe]^+$ and $[(bpg)Fe,CH_3OH]^+$, respectively [Eq. (2) and (3)], whereas the ion at m/z 342 is formed through an addition/elimination reaction involving $[(bpg\text{-}H)FeOH]^{+\bullet}$ isomer(s) [Eq. (4)].

$$[(bpg\text{-}H)FeOH]^{+\bullet} + ROH \rightleftharpoons [(bpg\text{-}H)FeOR]^{+\bullet} + H_2O \tag{4}$$

Kinetic plots for the formation of product ions through Equations (2) and (4) are shown in Figure 3b. About 4% of the precursor ion is depleted through methanol addition/water elimination [Eq. (4)] within 2 s, and is not depleted further at longer times (Figure 3b, open circles). In contrast, the kinetics for precursor depletion through O-atom transfer [Eq. (2)] is linear as a function of reaction time for the entire

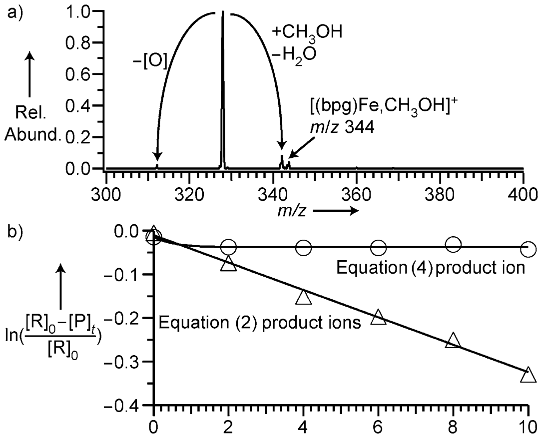

Figure 3. a) Mass spectrum obtained upon storing isolated $[(bpg)FeO]^+$ for 2 s in the presence of methanol (0.6×10^{-6} Torr), and b) kinetic plot (see Supporting Information for details) for the O-atom transfer reaction pathway [Eq. (2)] and addition/elimination reaction pathway [Eq. (4)].

range of reaction times (10 ms to 10 s). This data indicates that approximately 4 % of the *m*/*z* 328 ion population is the isomer(s) $[(bpg\text{-}H)FeOH]^{+\bullet}$ that is rapidly depleted through the reaction shown in Equation (4) within 2 s, whereas the remainder of the ion population is isomer **1**, which reacts more slowly through direct O-atom transfer to methanol [Eq. (2)].[16]

To gain insights into the addition/elimination reaction [Eq. (4)], we have carried out isotope labeling studies and allowed the product of addition/elimination to undergo ion–molecule reactions with water. When $[(bpg\text{-}H)FeOH]^{+\bullet}$ (*m*/*z* 328) was allowed to react with CD_3OH and $CH_3{}^{18}OH$ in separate experiments, isotopically unlabeled H_2O was predominantly lost upon addition of the respective methanol isotopologue (forming $[(bpg\text{-}H)FeOCD_3]^{+\bullet}$ (*m*/*z* 345) and $[(bpg\text{-}H)Fe^{18}OCH_3]^{+\bullet}$ (*m*/*z* 344), respectively). In contrast, the reaction with CH_3OD mainly results in the addition of the methanol isotopologue and the loss of HOD (Table S1). Thus for the water molecule that is lost through the reaction shown in Equation (4), the O atom and one H atom comes from the ion, while the other H atom comes from the O–H bond of the methanol substrate. This indicates that the methanol addition/water elimination reaction is a simple metathesis reaction that yields $[(bpg\text{-}H)FeOCH_3]^{+\bullet}$ [Eq. (4), $R=CH_3$]. $[(bpg\text{-}H)FeOCH_3]^{+\bullet}$ reacts with background water to give $[(bpg\text{-}H)FeOH]^{+\bullet}$ (*m*/*z* 328) [Eq. (4), back reaction], which suggests that the metathesis reaction is reversible.

Three potential mechanisms for the oxidation of primary alcohols by $[Fe^{IV}L]^+$, $L=bpg^-$ [Eq. (2)] or another suitable ligand, are shown in Scheme 1. These all yield the same product ion and neutrals, but differ by which of the three bonds is activated first and are based on related mechanisms proposed for methanol activation by $[Fe^{III}O]^+$.[9b] If the α-C–H bond is activated first (mechanism I) the formal oxidation state of Fe is reduced from IV to III to form a $Fe^{III}OH$/hydroxyalkyl radical complex, which can decompose through loss of H_2O and RCHO. If the O–H bond of the alcohol is activated first (mechanism II), a Fe^{IV} alkoxide and hydroxide intermediate $[LFe^{IV}(OH)(OCH_2R)]^+$ are formed, which can result in H_2O and RCHO elimination. If the C–O bond is activated first (mechanism III), the alkyl group can be transferred from the hydroxy group of RCH_2OH to the Fe=O group, to form the same $[LFe^{IV}(OH)(OCH_2R)]^+$ intermediate as for mechanism II.

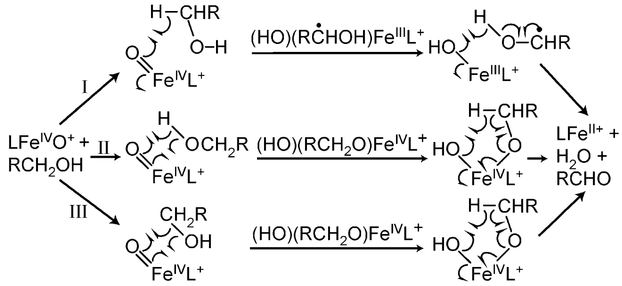

Scheme 1. Possible mechanisms for primary alcohol oxidation by a $Fe^{IV}O$ complex ion, where L is a ligand.

To exclude candidate mechanisms, rate constants were measured for the reactions of $[(bpg)Fe^{IV}O]^+$ with a range of isotopically labeled alcohols (CH_3OH, CD_3OH, CD_3OD and CH_3OD, CH_3CH_2OH, CH_3CD_2OH) under nearly identical conditions. Whereas $[(bpg)Fe^{IV}O]^+$ reacted with CH_3OH at a rate constant of $3.5\times10^{-13}\,cm^3\,molecules^{-1}\,s^{-1}$, in which only about 0.03 % of collisions resulted in O-atom transfer,[17] $[(bpg)Fe^{IV}O]^+$ reacted with CD_3OH about 20 times slower ($k_{exp}=1.8\times10^{-14}\,cm^3\,molecules^{-1}\,s^{-1}$), i.e., the kinetic isotope effect (k_H/k_D) is 20 ± 7. Similarly, $[(bpg)Fe^{IV}O]^+$ reacted with CD_3OD about 19 times slower than with CH_3OH. In contrast, $[(bpg)Fe^{IV}O]^+$ reacted with CH_3OD and CH_3OH with the same rate constant. The rate constant for the O-atom transfer to CH_3CH_2OH [Eq. (2)] by $[(bpg)Fe^{IV}O]^+$ ($4.2\times10^{-12}\,cm^3\,molecules^{-1}\,s^{-1}$, 0.3 % reaction efficiency) is 6 ± 2 times faster than that for CH_3CD_2OH ($6.9\times10^{-13}\,cm^3\,molecules^{-1}\,s^{-1}$). These results strongly indicate that the α-C–H bond of the alcohol substrate is activated by H abstraction by the Fe^{IV}=O group of the complex in the rate determining step, i.e., the alcohol molecule is oxidized through mechanism I. It is interesting that the weakest bond of the alcohol is not activated first.[18] C–H bond activation may occur first because the Fe atom, which has a large +IV/+III reduction potential, is reduced if the C–H bond is activated, whereas activation of the other bonds does not result in immediate Fe reduction.

What role does the bpg^- ligand play in methanol oxidation? The "bare" FeO cation, $[Fe^{III}O]^+$, reacts with methanol at 100 % efficiency under thermal conditions,[9a] which is well over 1000 times greater than that for $[(bpg)Fe^{IV}{=}O]^+$ reported here. However, the selectivity of methanol activation by $Fe^{III}O^+$ [Eqs. (5a)–(5d)] is less than that of $[(bpg)Fe^{IV}O]^+$. Thus, the addition of the bpg^- ligand to FeO^+ is a case in which the ligand addition enhances the selectivity of the reaction at the expense of reactivity.

$$[Fe^{III}O]^+ + CH_3OH \rightarrow [(HO)Fe(CH_2OH)]^+ + H^\bullet \tag{5a}$$

$$\rightarrow [\mathrm{Fe(CH_2O)}]^+ + \mathrm{H_2O} \qquad (5b)$$

$$\rightarrow [\mathrm{Fe(H_2O)}]^+ + \mathrm{CH_2O} \qquad (5c)$$

$$\rightarrow \mathrm{Fe}^+ + \mathrm{CH_2O} + \mathrm{H_2O} \qquad (5d)$$

Apparently, any enhancement of the reactivity of the Fe–oxo unit that occurs as a result of the *increased* formal oxidation state of Fe, for $[(\mathrm{bpg})\mathrm{Fe^{IV}{=}O}]^+$ vs. $\mathrm{Fe^{III}O^+}$, is offset by the steric protection and/or stabilization of the $\mathrm{FeO^+}$ unit resulting from the presence of the ligand. These results are consistent with the results for $(\mathrm{HO})\mathrm{Fe^{IV}{=}O^+}$, which reacts with methane with a rate constant that is about one half that for $\mathrm{Fe^{III}O^+}$.[9f] Also, the C–H bond activating capabilities of $\mathrm{FeO^+}$ are drastically reduced when ligated by $\mathrm{C_6H_6}$, $\mathrm{C_5H_5N}$, and $\mathrm{C_{10}H_8}$.[9c,d] Thus, "tuning" the properties of the fundamental $\mathrm{FeO^+}$ unit by ligation, even when the formal oxidation state of the Fe is increased, tends to decrease the Fe–oxo reactivity.

How does solvent influence alcohol oxidation by $\mathrm{Fe^{IV}O}$ species? Nam et al. investigated the oxidation of $\mathrm{PhCH_2OH}$ and $\mathrm{PhCD_2OH}$ by four different low-spin $\mathrm{Fe^{IV}{=}O}$ complexes, in which two were heme-bound complexes dissolved in butyronitrile and the other two were non-heme complexes dissolved in acetonitrile.[10b] Large kinetic isotope effects, ranging from 20 to 60, were measured for all four $\mathrm{Fe^{IV}O}$ complexes, indicating that the alcohol is oxidized through H abstraction from the α-C–H bond by the FeO group, which also occurs for $[(\mathrm{bpg})\mathrm{Fe^{IV}O}]^+$(g) (mechanism I, Scheme 1). Thus, for these few examples of alcohol oxidation by $\mathrm{Fe^{IV}O}$ complexes, the mechanism does not appear to depend on the identity of the complex, or even on whether the reaction occurs in the gas or the condensed phases.

This work highlights the fruitful interplay between synthetic inorganic chemistry and gas phase ion chemistry in generating, characterizing and probing the fundamental reactivity of a biomimetic high-spin $\mathrm{Fe^{IV}{=}O}$ complex in vacuo. It paves the way for further studies that explore ligand architecture and oxidation state effects on biomimetic Fe–oxo chemistry. Ultimately such collaborations may lead to the development of new high-valent Fe–oxo biomimetic complexes that can selectively and efficiently activate strong bonds in organic substrates.

Experimental Section

Ion–molecule reactions were performed on a Finnigan LCQ quadrupole ion trap mass spectrometer as described previously.[19] $[(\mathrm{bpg})\mathrm{FeOFe}(\mathrm{bpg})]^{2+}$, generated through ESI of 300 μM solutions containing $[(\mathrm{bpg})(\mathrm{H_2O})\mathrm{FeOFe}(\mathrm{H_2O})(\mathrm{bpg})](\mathrm{ClO_4})_2$[11] in $\mathrm{CH_2Cl_2{:}CH_3CN}$ (90:10), was mass selected and subjected to CID. The resultant product, $[(\mathrm{bpg})\mathrm{FeO}]^+$, was mass selected and allowed to undergo ion–molecule reactions with the neutral alcohol. ESI solutions were introduced into the mass spectrometer using a syringe pump (2–4 $\mu\mathrm{L\,min^{-1}}$) and by applying 4–5 kV to the ESI capillary relative to the heated capillary entrance to the mass spectrometer (100–150 °C). Details of kinetics experiments are described in the Supporting Information.

Accurate mass measurements of ions were performed using a Finnigan hybrid LTQ-Fourier transform ion cyclotron resonance (FT-ICR) mass spectrometer that was modified to inject a gaseous mixture containing He and a neutral reagent into the linear ion trap, such that the He pressure is ca. 5 mTorr and the reagent pressure is ca. 10^{-6} Torr in the ion trap (Supporting Information). Ions resulting from ion–molecule reactions and/or CID that are formed in the linear ion trap were transferred to the FT-ICR cell for accurate mass measurements. The diiron oxo-bridged ion was generated using similar ESI conditions as that for the LCQ mass spectrometer.

Theoretical calculations were performed using the Gaussian 09 software package.[20] Ion structures were optimized for a number of different spin multiplicities and starting geometries using density functional theory (DFT) with the unrestricted BP86 functional, and the standard 6-31+G* basis set for C, O, N and H atoms. For Fe, a MDF10 Stuttgart Dresden 10-electron effective core potential with a (8s7p6d)/[6s5p3d] contraction scheme[21] was used. For each optimized structure, 0 K single-point energy values and vibrational frequencies were calculated using unrestricted B3LYP with the same basis set scheme that was used for geometry optimization.

Received: March 28, 2011
Published online: June 29, 2011

Keywords: alcohols · biomimetic chemistry · C–H activation · gas-phase reactions · non-heme iron complexes

---

[1] B. A. Arndtsen, R. G. Bergman, T. A. Mobley, T. H. Peterson, *Acc. Chem. Res.* **1995**, *28*, 154–162.

[2] a) A. E. Shilov, G. B. Shul'pin, *Chem. Rev.* **1997**, *97*, 2879–2932; b) L. Que, Jr., W. B. Tolman, *Nature* **2008**, *455*, 333–340.

[3] a) B. Meunier, S. P. de Visser, S. Shaik, *Chem. Rev.* **2004**, *104*, 3947–3980; b) A. S. Hakemian, A. C. Rosenzweig, *Annu. Rev. Biochem.* **2007**, *76*, 223–241.

[4] C. Krebs, D. G. Fujimori, C. T. Walsh, J. M. Bollinger, Jr., *Acc. Chem. Res.* **2007**, *40*, 484–492.

[5] a) W. Nam, *Acc. Chem. Res.* **2007**, *40*, 522–531; b) L. Que, Jr., *Acc. Chem. Res.* **2007**, *40*, 493–500.

[6] For a review of non-heme $\mathrm{Fe^{IV}}$–oxo intermediates of enzymes, see Ref. [4].

[7] a) For reviews of $\mathrm{Fe^{IV}}$–oxo biomimetic complexes, see Ref. [5]; b) J.-U. Rohde, J.-H. In, M. H. Lim, W. W. Brennessel, M. R. Bukowski, A. Stubna, E. Münck, W. Nam, L. Que, Jr., *Science* **2003**, *299*, 1037–1039; c) M. H. Lim, J. U. Rohde, A. Stubna, M. R. Bukowski, M. Costas, R. Y. N. Ho, E. Munck, W. Nam, L. Que, *Proc. Natl. Acad. Sci. USA* **2003**, *100*, 3665–3670; d) J. Kaizer, E. J. Klinker, N. Y. Oh, J. U. Rohde, W. J. Song, A. Stubna, J. Kim, E. Munck, W. Nam, L. Que, *J. Am. Chem. Soc.* **2004**, *126*, 472–473.

[8] a) O. Pestovsky, S. Stoian, E. L. Bominaar, X. Shan, E. Münck, L. Que, Jr., A. Bakac, *Angew. Chem.* **2005**, *117*, 7031–7034; *Angew. Chem. Int. Ed.* **2005**, *44*, 6871–6874; b) J. England, M. Martinho, E. R. Farquhar, J. R. Frisch, E. L. Bominaar, E. Münck, L. Que, Jr., *Angew. Chem.* **2009**, *121*, 3676–3680; *Angew. Chem. Int. Ed.* **2009**, *48*, 3622–3626; c) D. C. Lacy, R. Gupta, K. L. Stone, J. Greaves, J. W. Ziller, M. P. Hendrich, A. S. Borovik, *J. Am. Chem. Soc.* **2010**, *132*, 12188–12190.

[9] a) D. Schröder, R. Wesendrup, C. A. Schalley, W. Zummack, H. Schwarz, *Helv. Chim. Acta* **1996**, *79*, 123–132; b) K. Yoshizawa, Y. Kagawa, *J. Phys. Chem. A* **2000**, *104*, 9347–9355; c) D. Stöckigt, H. Schwarz, *Chem. Ber.* **1994**, *127*, 2499–2503; d) D. Stöckigt, H. Schwarz, *Liebigs Ann.* **1995**, 429–431; e) D. Schröder, A. Fiedler, J. Schwarz, H. Schwarz, *Inorg. Chem.* **1994**, *33*, 5094–5100; f) D. Schröder, H. Schwarz, *Angew. Chem.* **1991**, *103*, 987–989; *Angew. Chem. Int. Ed. Engl.* **1991**, *30*, 991–993.

[10] a) Numerous studies have investigated the gas-phase oxidation of methanol by metal ions and complexes. For a review of the literature, see: H. Schwarz, *Angew. Chem.* **2011**, DOI: 10.1002/ange.201006424; *Angew. Chem. Int. Ed.* **2011**, DOI: 10.1002/anie.201006424; b) for examples of alcohol oxidation by non-heme $Fe^{IV}O$ biomimetic complexes in solution, see: N. Y. Oh, Y. Suh, M. J. Park, M. S. Seo, J. Kim, W. Nam, *Angew. Chem.* **2005**, *117*, 4307–4311; *Angew. Chem. Int. Ed.* **2005**, *44*, 4235–4239.

[11] M. N. Mortensen, B. Jensen, A. Hazell, A. D. Bond, C. J. McKenzie, *Dalton Trans.* **2004**, 3396–3402.

[12] $[(bpg)FeOFe(bpg)]^{2+}$ (*m*/*z* 320) and its fragments, including $[(bpg)Fe^{IV}O]^{+}$, undergo a series of other fragmentation reactions during the CID process. This is the reason why the abundances of $[(bpg)Fe^{IV}O]^{+}$ and $[(bpg)Fe^{II}]^{+}$ are not equivalent in Figure 1a. We have also examined the ion–molecule reactions of $[(bpg)Fe^{IV}O]^{+}$ and $[(bpg)FeOFe(bpg)]^{2+}$ with other organic substrates. Full details of these CID and ion–molecule reaction experiments will be discussed in detail in a subsequent paper.

[13] The issue of isomerization has also been considered for high valent iron nitrides formed through CID of iron(III) azide complexes; e.g., M. Schlangen, et al., *J. Am. Chem. Soc.* **2008**, *130*, 4285–4294.

[14] a) J. England, Y. Guo, E. R. Farquhar, V. G. Young, Jr., E. Münck, L. Que, Jr., *J. Am. Chem. Soc.* **2010**, *132*, 8635–8644; b) E. J. Klinker, J. Kaizer, W. W. Brennessel, N. L. Woodrum, C. J. Cramer, L. Que, Jr., *Angew. Chem.* **2005**, *117*, 3756–3760; *Angew. Chem. Int. Ed.* **2005**, *44*, 3690–3694.

[15] For ion–molecule reaction times of up to 10 s and neutral molecule pressures of ca. 1×10^{-6} Torr, these ions do not react appreciably with either hexane or cyclohexane indicating that these ions would not activate simpler hydrocarbons, such as methane.

[16] While our experiments provide evidence for the formation of different isomers, they do not reveal how the isomers are formed. Isomerization can occur after disproportionation or different isomers can be formed through different disproportionation reactions of $[(bpg)FeOFe(bpg)]^{2+}$. Note that the minor isomer can be essentially "purged" from the ion trap by using higher alcohol pressures and/or a longer time delay between the formation of the *m*/*z* 328 ion population and isolation of this ion population.

[17] For a k_{col} value of $1.4\times10^{-9}\,cm^3\,molecules^{-1}\,s^{-1}$ that was calculated using ADO theory (see Experimental Section).

[18] The C–H, O–H, and C–O bond dissociation energies of methanol are 414.0, 440.0, and 389.7 $kJ\,mol^{-1}$, respectively.

[19] T. Waters, R. A. J. O'Hair, A. G. Wedd, *J. Am. Chem. Soc.* **2003**, *125*, 3384–3396.

[20] Gaussian 09; M. J. Frisch et al., Gaussian, Inc., Wallingford, CT, **2009**.

[21] M. Dolg, U. Wedig, H. Stoll, H. Preuss, *J. Chem. Phys.* **1987**, *86*, 866–872.